

Local molecular field theory for effective attractions between like charged objects in systems with strong Coulomb interactions

Yng-Gwei Chen^{1,3,*} and John D. Weeks^{2,3}

¹*Department of Physics,* ²*Department of Chemistry and Biochemistry,*
and ³*Institute for Physical Science and Technology,*
University of Maryland, College Park, Maryland 20742

Strong short ranged positional correlations involving counterions can induce a net attractive force between negatively charged strands of DNA, and lead to the formation of ion pairs in dilute ionic solutions. But the long range of the Coulomb interactions impedes the development of a simple local picture. We address this general problem by mapping the properties of a nonuniform system with Coulomb interactions onto those of a simpler system with short ranged intermolecular interactions in an effective external field that accounts for the averaged effects of appropriately chosen long ranged and slowly varying components of the Coulomb interactions. The remaining short ranged components combine with the other molecular core interactions and strongly affect pair correlations in dense or strongly coupled systems. We show that pair correlation functions in the effective short ranged system closely resemble those in the uniform primitive model of ionic solutions, and illustrate the formation of ion pairs and clusters at low densities. The theory accurately describes detailed features of the effective attraction between two equally charged walls at strong coupling and intermediate separations of the walls. New analytical results for the minimal coupling strength needed to get any attraction and for the separation where the attractive force is a maximum are presented.

Strong Coulomb interactions in crowded nonuniform environments have important experimental consequences in a wide variety of biophysical applications ranging from DNA packaging in viruses to transport in ion channels [1, 2, 3, 4]. They present major challenges to theory and computer simulations not only because of their characteristic long range but also because they can be very strong at short distances. We present here a new local molecular field (LMF) theory [5] that averages over particular long ranged and slowly varying components of the Coulomb interactions [6] while still maintaining an accurate description of the short ranged components. It provides a general and physically suggestive theory for strongly coupled Coulomb systems and reduces exactly to the classical Poisson-Boltzmann (PB) approximation for dilute weakly coupled systems.

We consider a general starting point where a molecule of species i , described by a rigid body frame with center at \mathbf{r}_i , interacts with an external field $\phi_{fi}(\mathbf{r}_i)$ that comes

from fixed charged solutes, or walls, or particular fixed molecules of a mobile species, as illustrated below. The subscript f indicates the source of the field, which we treat as a special fixed species f . The interaction between a pair of molecules of species i and j is assumed to have the general form $w_{ij}(\mathbf{r}_{ij}) = w_{s,ij}(\mathbf{r}_{ij}) + w_{q,ij}(\mathbf{r}_{ij})$, where $\mathbf{r}_{ij} \equiv \mathbf{r}_j - \mathbf{r}_i$. The $w_{s,ij}(\mathbf{r}_{ij})$ denote general (repulsive core and other) short ranged intermolecular interactions. There are angular coordinates expressing orientations of the body frames that we do not denote explicitly. The $w_{q,ij}(\mathbf{r}_{ij})$ arise from Coulomb interactions between rigid charge distributions $q_i(\mathbf{r}-\mathbf{r}_i)$ in the body frame of each molecule, so that

$$w_{q,ij}(\mathbf{r}_{ij}) = \int d\mathbf{r} \int d\mathbf{r}' \frac{q_i(\mathbf{r}-\mathbf{r}_i)q_j(\mathbf{r}'-\mathbf{r}_j)}{\epsilon|\mathbf{r}-\mathbf{r}'|} \quad (1)$$

$$= \frac{1}{(2\pi)^3} \int d\mathbf{k} \hat{q}_i(-\mathbf{k})\hat{q}_j(\mathbf{k})e^{-i\mathbf{k}\cdot\mathbf{r}_{ij}} \frac{4\pi}{\epsilon k^2}, \quad (2)$$

where the caret denotes a Fourier transform and we assume there is a uniform dielectric constant ϵ everywhere.

To generate uniformly slowly varying components $u_{1,ij}$ of the full $w_{q,ij} \equiv w_{q0,ij} + u_{1,ij}$ that are well suited for LMF averaging, we limit the magnitude of wave vectors making significant contributions to the integration in Eq. 2. To that end we introduce a Gaussian function parameterized by an important length scale σ that provides a smooth cutoff in k -space, and write

$$\frac{4\pi}{k^2} = \frac{4\pi}{k^2} e^{-\frac{1}{4}(k\sigma)^2} + \frac{4\pi}{k^2} (1 - e^{-\frac{1}{4}(k\sigma)^2}). \quad (3)$$

The first term on the right has all the characteristic long ranged Coulomb divergences as $k \rightarrow 0$, but decays very rapidly to zero for $k\sigma \gtrsim 2$. The desired slowly varying components arise when only this term is used in Eq. 2 with an appropriate choice of σ . For localized charge distributions $\hat{q}_i(\mathbf{k})$ we expand in a Taylor series about $\mathbf{k} = 0$ and take the lowest order multipole moment [7]. This simplified expression defines the $u_{1,ij}$ we consider and

Abbreviations: LMF, local molecular field; PB Poisson-Boltzmann; SAPM size asymmetric primitive model; WL Weis and Levesque; MC Monte Carlo; SCA strong coupling approximation; mPB mimic Poisson-Boltzmann

* Present address: Laboratory of Chemical Physics and National Institute of Diabetes and Digestive and Kidney Diseases, Bldg. 5, National Institutes of Health, Bethesda, MD 20892

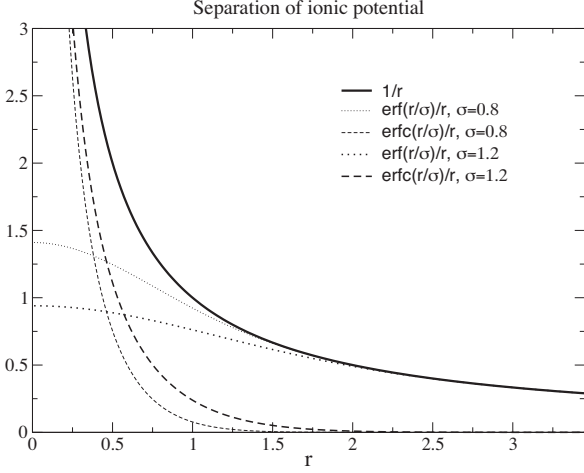


FIG. 1: Separation of the $1/r$ potential into a slowly varying piece $\text{erf}(r/\sigma)/r$ and the short ranged remainder $\text{erfc}(r/\sigma)/r$. Two relevant σ values are shown; a bigger σ generates a more slowly varying long ranged component.

thus prescribes a σ -dependent separation of the full intermolecular potentials $w_{ij}(\mathbf{r}_{ij}) = w_{s,ij}(\mathbf{r}_{ij}) + w_{q,ij}(\mathbf{r}_{ij}) = w_{s,ij}(\mathbf{r}_{ij}) + w_{q0,ij}(\mathbf{r}_{ij}) + u_{1,ij}(\mathbf{r}_{ij}) \equiv u_{0,ij}(\mathbf{r}_{ij}) + u_{1,ij}(\mathbf{r}_{ij})$ into short and long ranged parts.

In r -space Eq. 3 becomes $1/r = \text{erf}(r/\sigma)/r + \text{erfc}(r/\sigma)/r$. Here erf and erfc are the usual error and complementary error functions. The $\text{erf}(r/\sigma)/r$ term is the electrostatic potential from a normalized Gaussian charge distribution with width σ . As shown in Fig. 1, this remains smooth and slowly varying on the scale of σ , while decaying as $1/r$ at large r . This use of a Gaussian charge distribution is related to the Ewald sum method, which considers periodic images of ion configurations with embedded screening and compensating Gaussian charge distributions. However, our focus is on the separation of the potential itself and not the effects of periodic boundary conditions and our choice of σ is usually much smaller than that used in Ewald sum methods, which typically is proportional to the width of the simulation cell [8].

The short ranged components $u_{0,ij}(\mathbf{r}_{ij})$ define the intermolecular interactions in the special short ranged “mimic system”. They are comprised of the short ranged parts of the Coulomb interactions $w_{q0,ij} \equiv w_{q,ij} - u_{1,ij}$ and the other short ranged core interactions $w_{s,ij}$:

$$u_{0,ij}(\mathbf{r}_{ij}) \equiv w_{s,ij}(\mathbf{r}_{ij}) + w_{q0,ij}(\mathbf{r}_{ij}). \quad (4)$$

As suggested by Fig. 1, σ sets the range of $w_{q0,ij}$ and thus determines an effective Coulomb core size [6]. The external potential from fixed charged solutes or walls $\phi_{fi}(\mathbf{r}_i) \equiv \phi_{0,fi}(\mathbf{r}_i) + \phi_{1,fi}(\mathbf{r}_i)$ can similarly be separated into short and long ranged parts, as illustrated below.

It is straightforward to arrive at explicit results for the $u_{1,ij}(\mathbf{r})$ and $\phi_{1,fi}(\mathbf{r}_i)$. Here we consider localized charge distributions with a net charge $\bar{q}_i \equiv \int d\mathbf{r} q_i(\mathbf{r})$ or a net dipole moment $\mathbf{p}_i \equiv \int d\mathbf{r} \mathbf{r} q_i(\mathbf{r})$. If both molecules carry a net charge we find

$u_{1,ij}(r) = \bar{q}_i \bar{q}_j \text{erf}(r/\sigma)/\epsilon r$. The associated Coulomb core component is $w_{q0,ij} = \bar{q}_i \bar{q}_j \text{erfc}(r/\sigma)/\epsilon r$. Thus the results of Fig. 1, scaled by $\bar{q}_i \bar{q}_j/\epsilon$, give examples of possible $u_{1,ij}$ and $w_{q0,ij}$ for ionic solution models [6]. For a monopole and a dipole we find $u_{1,ij}(\mathbf{r}) = \bar{q}_i (\mathbf{p}_j \cdot \nabla) [\text{erf}(r/\sigma)/\epsilon r]$, and for dipoles $u_{1,ij}(\mathbf{r}) = -(\mathbf{p}_i \cdot \nabla)(\mathbf{p}_j \cdot \nabla) [\text{erf}(r/\sigma)/\epsilon r]$. The latter will lead to dipolar mimic systems with short ranged angular dependent interactions.

Local molecular field approximation

LMF theory introduces renormalized effective fields $\phi_{R,fi}(\mathbf{r}_i)$ that induce nonuniform singlet densities in the mimic system (denoted by the subscript R) that are supposed to equal those induced by the $\phi_{fi}(\mathbf{r}_i)$ in full system of interest:

$$\rho_{R,fi}(\mathbf{r}_i) = \rho_{fi}(\mathbf{r}_i). \quad (5)$$

This defines a general mapping relating structure in the mimic and full systems. Thermodynamic properties can be determined by integration of these structural relations.

We represent the effective field $\phi_{R,fi}(\mathbf{r}_i) \equiv \phi_{0,fi}(\mathbf{r}_i) + \phi_{R1,fi}(\mathbf{r}_i)$ as the sum of the known short ranged part $\phi_{0,fi}(\mathbf{r}_i)$ of the external field in the full system and a renormalized “perturbation component” $\phi_{R1,fi}(\mathbf{r}_i)$ that accounts for the averaged effects of the slowly varying interactions $u_{1,ij}$. As discussed in detail in [5, 6], by considering the balance of forces in the full and mimic systems when Eq. 5 holds, and making some physically motivated approximations, we find that the $\phi_{R1,fi}$ are determined up to a constant by the *local molecular field equations*:

$$\phi_{R1,fi}(\mathbf{r}_i) = \int' d\mathbf{r}_j [\delta(f, j) + \rho_{R,fj}(\mathbf{r}_j)] u_{1,ji}(\mathbf{r}_{ji}). \quad (6)$$

Here the prime on the integral indicates an implicit summation over all species j and an integration over the angles of the body frames. Long ranged interactions from the fixed species f are accounted for by the $\delta(f, j)$ term, which denotes products of δ -functions describing the fixed location and orientation of f .

Note that the average over the slowly varying $u_{1,ji}(\mathbf{r}_{ji})$ in Eq. 6 is weighted by $\rho_{R,fj}(\mathbf{r}_j)$, the *singlet* density for species j (in the effective field of fixed species f but with no explicit reference to species i). This neglect of pair correlations between molecules at \mathbf{r}_j and \mathbf{r}_i characterizes a mean field approximation [2], and in most contexts this would represent a major source of error. However, a general feature illustrated by Fig. 1 is that as σ increases the $u_{1,ji}$ become progressively more slowly varying at short distances. Thus we can ensure that all the $u_{1,ji}$ will be slowly varying over the length scales of relevant local pair correlations in the system by choosing σ larger than some state dependent minimum value σ_{\min} . This permits a consistent and controlled use of the mean field approximation in computing the average, and we anticipate very accurate results from the LMF theory for any

$\sigma \geq \sigma_{\min}$ if we properly describe the resulting density in the mimic system [6].

At strong coupling we argue that σ_{\min} should be of order a characteristic nearest neighbor spacing \bar{a} . The strong short ranged parts of the Coulomb interactions on the scale of \bar{a} and below directly affect pair correlations between nearest neighbor molecules. These will be consistently described in the mimic system if we choose $\sigma = \sigma_{\min}$ of order \bar{a} so that there are essentially nearest neighbor interactions between the effective Coulomb cores and the averaged effects of the $u_{1,ji}$ from the further neighbors are slowly varying on this scale. We illustrate below the utility of these ideas for simple models of ionic solutions at strong coupling.

Size-asymmetric primitive model

A model of great current interest is the size-asymmetric primitive model (SAPM) of ionic solutions, a fluid of oppositely charged hard spheres of different sizes in a uniform dielectric continuum. The different hard sphere diameters crudely account for the different core sizes of real cations and anions, and there is an interesting and not well-understood dependence of the critical temperature and critical density in this model as the size or charge ratio is varied [9]. We consider in particular the uniform equimolar system studied using Monte Carlo (MC) simulations [10] by Weis and Levesque (WL), with symmetric unit charges $e_0 = \bar{q}_1 = -\bar{q}_2$ and a diameter ratio $d_1/d_2 = 0.4$. Thus $w_{s,ij}(r) = \infty$ for $r \leq d_{ij} \equiv (d_i + d_j)/2$, and is zero otherwise, and $w_{q,ij}(r) = \bar{q}_i \bar{q}_j / \epsilon r$.

WL characterize the states by two dimensionless parameters: a reduced density $\rho^* \equiv (N_1 + N_2)d_2^3/V$ and an effective coupling strength $\Gamma^* \equiv l_B/d_2$ (called q^{*2} in the notation of WL). Here $l_B \equiv \beta e_0^2/\epsilon$ is the *Bjerrum length*, the distance where the interaction energy between two unit charges e_0 equals $k_B T$, and $\beta \equiv (k_B T)^{-1}$. Their simulations indicate that the critical point occurs at $\rho^* = 0.195$ and $\Gamma^* = 15.15$. We report results here for two strong coupling states with very different properties: a high density subcritical liquid state with $\rho^* = 1.4$ and $\Gamma^* = 16$, and a low density supercritical vapor state with $\rho^* = 0.04$ and $\Gamma^* = 9$.

The competition between the Coulomb interactions and the packing arrangements of the embedded hard cores in the SAPM produces elaborate local structures in these strong coupling states as exhibited in the pair correlation functions $g_{ij}(r)$, proportional to the density response to an external field $\phi_{ij}(r) = w_{ij}(r)$ arising from a fixed ion of type i at the origin. Thus in LMF theory even uniform fluid correlation functions are described from a nonuniform point of view. These characteristic features can be very accurately reproduced in the mimic system using the *strong coupling approximation* (SCA). The SCA replaces $\phi_{R,ij}(r)$ by the known strong short ranged component $\phi_{0,ij}(r) = u_{0,ij}(r)$ of the field from fixed ion i . This corresponds to fixing a mimic particle at the origin, or equivalently, approximating the $g_{ij}(r)$ in the uniform ionic system by the $g_{0,ij}(r)$ in the uniform

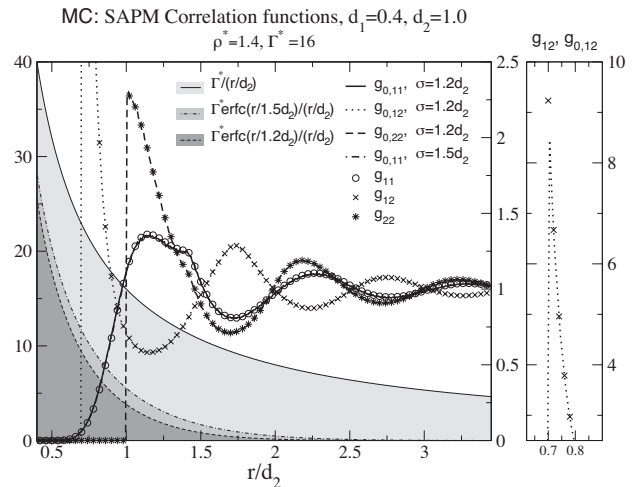


FIG. 2: Dimensionless potentials and pair correlation functions for the SAPM at high density and strong coupling. The potentials use the left vertical axis. Both the full potential between positive ions (light grey shading) and the mimic interactions for two different values of σ (darker grey shadings) are shown. The various pair correlation functions use the right vertical axis. Results for $g_{0,11}$ using two different values of σ are shown; the differences are barely visible on the scale of the graph. The right inset focuses on the high first peak of the cation-anion correlation function.

mimic system [6].

In Fig. 2 we compare correlation functions determined by WL for the high density state with $\rho^* = 1.4$ and $\Gamma^* = 16$ to MC simulations we carried out in the uniform mimic system with a “molecular sized” choice of $\sigma = 1.2d_2$ using the SCA. Simulations of the long ranged system required careful and costly treatment of periodic boundary conditions using the Ewald sum method; this was not needed for the short ranged mimic system. Despite the very different range and magnitude of the mimic system interactions, all the pair correlation functions are strikingly similar to those of the full SAPM. These functions are very different from the profiles of the associated hard sphere mixture with the charges set equal to zero, indicating the crucial importance of including the strong short ranged parts of the Coulomb interactions $w_{q0,ij}$ in defining the mimic interactions in Eq. 4. Equally good results are found for larger values of σ , as illustrated in the figure, but the good agreement fails for much smaller σ , indicating that σ_{\min} is about $1.2d_2$ for this state.

Qualitatively different structures are seen in the low density vapor state with $\rho^* = 0.04$, and $\Gamma^* = 9$, as illustrated in Fig. 3. The simulations of WL show that oppositely charged ions pair together with a typical spacing close to the minimum permitted by the hard core diameters, along with some transient formation of longer chain-like structures. The correlation functions between like-charged pairs exhibit pronounced peaks of essentially the same magnitude at a separation of $r = 1.4d_2 = d_1 + d_2$. This indicates the existence of small clusters of ion pairs, with the same peak position and amplitude for both

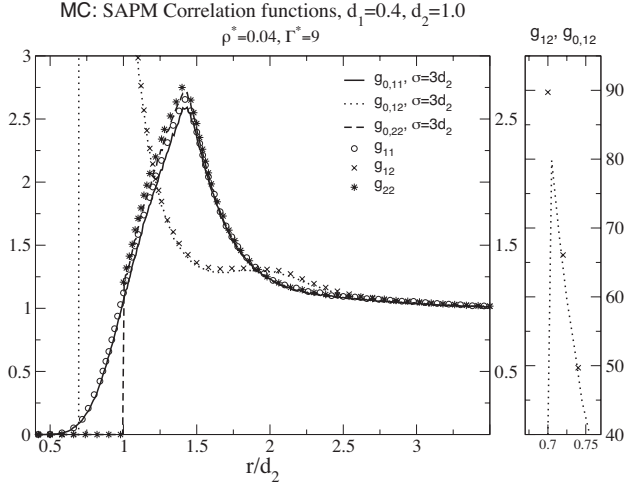


FIG. 3: Pair correlation functions for the SAPM in the low density ion pairing regime, with the same conventions as in Fig. 2.

“+ − +” or “− + −” configurations at the minimum distance permitted by a linear arrangement of the embedded hard cores. These peaks also illustrate how counterions can induce an effective attraction between like charged objects, as discussed in detail in the next section. Very good agreement between full and mimic system correlation functions is achieved with a choice of $\sigma_{\min} = 3.0d_2$, consistent with the larger average spacing between dilute ion pairs.

The clustering of the ions has probably presented the most severe challenges to theories of ionic systems. It is particularly crucial for the study of critical phenomena and vapor-liquid coexistence [9]. The PB approximation and the frequently used hypernetted chain (HNC) integral equation fail to predict ion clustering; indeed the HNC equation has no solution in most of the ion pairing regime [10]. In contrast, the mimic system as described by the simple SCA already builds in the most important local features of ion aggregation. This very good agreement strongly suggests that the LMF theory can accurately represent the Coulomb cores that contribute to local correlation functions in more realistic models of ionic systems. Any remaining errors can be attributed mainly to deficiencies in the description of the other short ranged core interactions, thus permitting the efficient development of more accurate models.

Charged walls with point counterions

The suspension and self-assembly of highly charged polyelectrolytes (macroions) in the presence of mobile counterions (microions) is of great interest in biological systems [1]. These systems usually involve charge and size asymmetries much greater than that of the SAPM and are often studied by fixing a certain macroion configuration and computing the microion distribution and resulting forces on the macroions. We discuss here the simplest such model system [11], consisting of

uniformly charged infinite hard walls with neutralizing point counterions (and no co-ions) in a uniform dielectric environment. This model is simple enough that exact results in certain limits are known [12], but it still illustrates many fundamental issues that arise from the interplay between long and short ranged forces in an explicitly nonuniform environment. It is clear from the previous section that the LMF theory can deal with more realistic models for the walls and counterions.

One charged wall We first consider the case of a single hard wall with a uniform negative charge density q_w at the $z = 0$ plane, where we take the zero of electric potential energy. Without loss of generality we can assume that the counterions have a (unit) charge e_0 and express the wall charge density $q_w \equiv -e_0/l_w^2$ in terms of the length l_w of the side of a square enclosing that amount of charge. The potential energy $\phi^{1w}(z)$ of a counterion at a distance z from the wall is $2\pi e_0^2 z / (\epsilon l_w^2)$. The *Gouy-Chapman length* l_G is defined as the distance where this potential equals $k_B T$, i.e., $l_G \equiv k_B T \epsilon l_w^2 / (2\pi e_0^2) = l_w^2 / (2\pi l_B)$. l_G characterizes the effective strength of the attractive wall-counterion interaction, and most counterions will be found near the wall in an effective slit whose width is proportional to l_G . Dimensionless combinations of thermodynamic variables in this simple system depend only on a single control parameter [13] $\xi \equiv l_B / l_G = l_w^2 / (2\pi l_G^2)$.

As ξ increases (e.g., by decreasing T at fixed wall and counterion charge) counterions are driven increasingly close to the wall by the decreasing l_G . At strong coupling with $\xi \gg 1$ or $l_G \ll l_w$, most counterions are next to the wall and form a (“strongly-correlated”) two dimensional (2D) liquid layer [14, 15] with average lateral spacing $\bar{a} \simeq a_{2D} \equiv l_w$ fixed by local neutrality. There are indeed strong lateral correlations between the counterions in the 2D layer: the coupling strength $\Gamma_{a_{2D}} \equiv l_B / a_{2D} = \xi^{1/2} / (2\pi)^{1/2} \gg 1$ for large ξ . As discussed above we then expect the effective Coulomb core size σ_{\min} to be of order $a_{2D} = l_w$. However, because of these repulsive cores, particles cannot stack perpendicular to the wall and remain near the narrow slit. Thus the density outside the slit is very low and there are only weak correlations normal to the wall.

In the opposite weak coupling limit with $\xi \ll 1$ or $l_G \gg l_w$ counterions can take advantage of the larger effective volume of the slit and adopt a more diffuse 3D packing to reduce their repulsive interactions. Crudely assuming all counterions are found within l_G of the wall and using a simple cubic lattice to estimate the characteristic counterion spacing in this volume we now have $\bar{a} \simeq a_{3D} \equiv (l_w^2 l_G)^{1/3} = l_w / (2\pi \xi)^{1/6}$. There is weak coupling between the counterions, with $\Gamma_{a_{3D}} \equiv l_B / a_{3D} = \xi^{2/3} / (2\pi)^{1/3} \ll 1$ and here it is natural to take $\sigma_{\min} \simeq l_B = l_w (\xi / 2\pi)^{1/2}$ as an estimate for the effective Coulomb core size [6]. The crossover to strong coupling with essentially 2D packing and $\sigma_{\min} \simeq a_{2D} = l_w$ occurs for ξ of order unity, and the 2D packing indeed provides a larger average spacing at

large ξ .

Quantitative results take an especially simple form [13] if we introduce a dimensionless rescaled density $n(z/l_G) \equiv l_G l_w^2 \rho(z)$ that incorporates the anticipated (ξ -dependent) scaling of the profile with l_G . Local neutrality requires that $\int_0^\infty d\tilde{z} n(\tilde{z}) = 1$, where $\tilde{z} \equiv z/l_G$. Lengths scaled by l_G will generally be indicated by a tilde. Moreover, because of the impulsive δ -function force at a hard wall, there is an exact relation between the pressure and the contact density. This yields the well-known *contact theorem*, which implies $n(0) = 1$ for the contact value of the rescaled density at a single charged hard wall [11].

Exact results [12] for $n(\tilde{z})$ are known in the limit $\xi \rightarrow 0$ from a rigorous weak coupling expansion, which gives results agreeing with the PB approximation, $n_{PB}(\tilde{z}) = 1/(\tilde{z} + 1)^2$. A different strong coupling expansion gives exact results as $\xi \rightarrow \infty$, $n_{SC}(\tilde{z}) = e^{-\tilde{z}}$. However, attempts to connect these limits by analyzing higher order terms in each expansion have had only limited success [13]. We now show that the LMF theory provides a simple, accurate, and unified approach for general ξ .

LMF equation for one charged wall We can take advantage of planar symmetry and integrate exactly over the lateral degrees of freedom in the long ranged parts $u_{1,ji}(\mathbf{r}_{ji})$ of the counterion-counterion and wall-counterion interactions in Eq. 6. The resulting LMF equation can be written in dimensionless form for $\tilde{z}_1, \tilde{z}_2 \geq 0$ as

$$\tilde{\phi}_{R1}(\tilde{z}_1) = \int_0^\infty d\tilde{z}_2 [-\delta(\tilde{z}_2) + n_R(\tilde{z}_2)] G(\tilde{z}_2, \tilde{z}_1). \quad (7)$$

Here $\tilde{\phi}_{R1}(\tilde{z}_1) \equiv \beta \phi_{R1}(\tilde{z}_1 l_G)$ and $G(\tilde{z}_2, \tilde{z}_1) \equiv -|\tilde{z}_1 - \tilde{z}_2| \text{erf}(|\tilde{z}_1 - \tilde{z}_2|/\tilde{\sigma}) - \pi^{-1/2} \tilde{\sigma} e^{-[(\tilde{z}_1 - \tilde{z}_2)/\tilde{\sigma}]^2} + |\tilde{z}_2| \text{erf}(|\tilde{z}_2|/\tilde{\sigma}) + \pi^{-1/2} \tilde{\sigma} e^{-[\tilde{z}_2/\tilde{\sigma}]^2}$ is the Green's function associated with a normalized planar Gaussian charge distribution centered at \tilde{z}_2 , with the zero of potential energy at $\tilde{z}_1 = 0$.

The $-\delta(\tilde{z}_2)$ term in Eq. 7 accounts for the long ranged component $\tilde{\phi}_1(\tilde{z}_1) = -G(0, \tilde{z}_1)$ of the dimensionless attractive potential $\tilde{\phi}^{1w}(\tilde{z}_1) = \tilde{z}_1$ between a counterion at \tilde{z}_1 and the negatively charged wall at $\tilde{z}_2 = 0$. The remaining short ranged part $\tilde{\phi}_0(\tilde{z}_1) = \tilde{z}_1 - \tilde{\phi}_1(\tilde{z}_1)$ of the wall potential is

$$\tilde{\phi}_0(\tilde{z}_1) = \tilde{z}_1 \text{erfc}(\tilde{z}_1/\tilde{\sigma}) - \tilde{\sigma} e^{-(\tilde{z}_1/\tilde{\sigma})^2} / \sqrt{\pi} + \tilde{\sigma} / \sqrt{\pi}. \quad (8)$$

The effective field is then $\tilde{\phi}_R(\tilde{z}_1) = \tilde{\phi}_0(\tilde{z}_1) + \tilde{\phi}_{R1}(\tilde{z}_1)$, with $\tilde{\phi}_{R1}$ given by Eq. 7 for $\tilde{z}_1 \geq 0$, and infinity otherwise.

mPB approximation To solve Eq. 7 self consistently we must accurately determine the density $n_R(\tilde{z})$ induced by $\tilde{\phi}_R(\tilde{z})$. At weak coupling, neighboring ions interact weakly and the density response to the effective field is proportional to the ideal gas Boltzmann factor $\exp[-\tilde{\phi}_R(\tilde{z})]$. Using this approximation in Eq. 7, we have a closed equation, which we refer to as the *mimic*

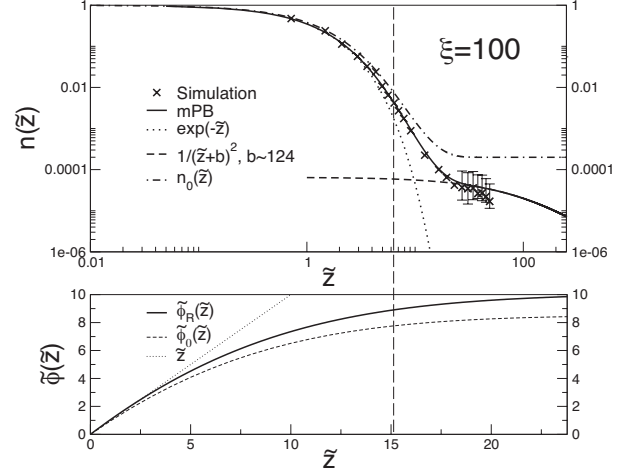


FIG. 4: Upper graph: (Note the log scales) Rescaled counterion density near one planar charged wall calculated by the full mPB theory and by the SCA compared to computer simulation data in [13]. The limiting exponential profile provides a good fit only near the wall. We can show analytically [7] that there is a crossover to an algebraic tail of the form $1/(\tilde{z} + b)^2$ in the mPB theory for $\tilde{z} \simeq \tilde{\sigma}^{1w}$ as seen in the graph. The vertical dashed line in both graphs indicates the value of $\tilde{\sigma}^{1w}$. Lower graph: (Note the linear scales) The full dimensionless wall potential \tilde{z} compared to $\tilde{\phi}_R(\tilde{z})$ and $\tilde{\phi}_0(\tilde{z})$ from the mPB theory.

Poisson-Boltzmann (mPB) equation. Moreover, we can show [7] for all ξ that a self consistent solution of the mPB equation will exactly satisfy both neutrality and the contact theorem. The latter implies that the density response takes the simple form $n_R(\tilde{z}) = \exp[-\tilde{\phi}_R(\tilde{z})]$ with our choice of zero of energy.

Remarkably, however, the mPB approximation also gives accurate results at *strong coupling* with $\xi \gg 1$, where there is an essentially 2D arrangement of the mimic particles in an effective narrow slit. Correlations normal to the wall are very weak and the Boltzmann factor again can accurately describe the density response to the z -dependent field $\tilde{\phi}_R(\tilde{z})$, as can be verified by more formal arguments [13, 16].

This motivates our use of the mPB approximation with $n_R(\tilde{z}) = \exp[-\tilde{\phi}_R(\tilde{z})]$ for all ξ in Eq. 7. The mPB approximation is least justified at intermediate values of ξ , and it breaks down if σ is chosen much larger than σ_{\min} so that there would be strong direct interactions between further neighbors in the mimic system. Thus we provide a smooth interpolation between the known limiting values of σ_{\min} in the weak and strong coupling regimes by choosing $\sigma = \sigma^{1w} \equiv C \min(l_B, l_w)$, and fix $C = 0.60$ by finding the best fit to simulations [13] at a moderately strong coupling state with $\xi = 40$. In this example it is numerically more convenient to differentiate the resulting mPB equation and solve for the effective force, which vanishes far from the wall, and then get the effective field by integration [17]. An iterative solution is straightforward and no other

simulation data are required.

Results for one charged wall Figure 4 gives results for $n_R(\tilde{z})$ at strong coupling with $\xi = 100$. There is excellent agreement between the results of the mPB theory and MC simulations [13] of the long ranged system carried out by Moreira and Netz. The log-log plot emphasizes that $n_R(\tilde{z})$ has two characteristic regions. Near the wall there is an initial exponential decay arising mainly from particles in the 2D layer. This continues until about $\tilde{z} \simeq \tilde{\sigma}_{\min}/2$ where the density is very low and there is a crossover to algebraic decay as in the PB solution, but with a much larger effective l_G . A natural physical interpretation is that the small fraction of counterions outside the 2D layer adopt a diffuse PB-like profile generated by an effective wall whose charge density has been greatly reduced by the charge of the tightly bound counterions. This idea has been suggested before [15], but LMF theory is the first unified theory capable of describing both limiting regions and the crossover region.

The density near the wall is very accurately described by the even simpler SCA, where $\phi_R(\tilde{z})$ is approximated by $\tilde{\phi}_0(\tilde{z})$. The resulting density $n_0(\tilde{z}) \equiv \exp[-\tilde{\phi}_0(\tilde{z})]$ can be written down immediately from Eq. 8. As shown in Fig. 4 both $\tilde{\phi}_0(\tilde{z})$ and $\phi_R(\tilde{z})$ closely resemble the full potential \tilde{z}_1 near the wall for $\tilde{z}_1 \lesssim \tilde{\sigma}_{\min}/2$. But $n_0(\tilde{z})$ cannot describe the PB-like region at large \tilde{z} as does the full mPB theory and it does not obey the neutrality condition. This example highlights both the strengths and weaknesses of the SCA. When properly used to describe only short ranged correlations at strong coupling very accurate results can be found.

Two charged walls We now briefly consider two equally charged hard walls forming a real slit with width d , with neutralizing point counterions in between. At strong coupling and intermediate widths, the counterions can induce an effective attractive force between the walls. Such effective attraction between like charged objects may have important experimental consequences, and it has generated a great deal of theoretical interest [1, 2, 3, 4].

Reference [11] gives an exact expression for the dimensionless (osmotic) pressure $\tilde{P} \equiv \beta l_G l_w^2 P$ arising from neutralizing point counterions confined between charged hard walls at $z = 0$ and $z = d$:

$$\tilde{P} = n(0) - 1. \quad (9)$$

Thus if the rescaled contact density $n(0)$ is less than (greater than) one there is an effective attractive (repulsive) force on the walls. As $d \rightarrow \infty$, we recover the one-wall results discussed earlier, where $\tilde{P} = 0$, and $n(0) = 1$.

Since the total force on a counterion from equally charged walls exactly cancels for all z and all d , we now have $\tilde{\phi}^{2w}(\tilde{z}) = 0$ for $0 \leq \tilde{z} \leq \tilde{d}$. As in the one-wall case,

it is useful to divide $\tilde{\phi}^{2w}$ into a short ranged part

$$\tilde{\phi}_0^{2w}(\tilde{z}; \tilde{d}) \equiv \tilde{\phi}_0^{1w}(\tilde{z}) + \tilde{\phi}_0^{1w}(\tilde{d} - \tilde{z}) - \tilde{\phi}_0^{1w}(\tilde{d}), \quad (10)$$

given by a sum of short ranged single-wall terms (indicated by the superscript $1w$) defined in Eq. 8, and the remainder. We take the zero of energy on the left wall at $\tilde{z} = 0$. The effective field $\tilde{\phi}_R(\tilde{z}) = \tilde{\phi}_0^{2w}(\tilde{z}; \tilde{d}) + \tilde{\phi}_{R1}(\tilde{z})$ is determined from the two-wall LMF equation. This closely resembles Eq. 7, except that the integration is from 0 to \tilde{d} and there is an additional $-\delta(\tilde{d} - \tilde{z}_2)$ term in the integrand, accounting for interactions with the second wall at $z = d$. Again we use the mPB approximation $n_R(\tilde{z}) = A \exp[-\phi_R(\tilde{z})]$ and fix the constant A (which equals the contact density with our choice of zero of energy) using the neutrality condition $\int_0^{\tilde{d}} d\tilde{z} n_R(\tilde{z}) = 2$. The pressure is then given by Eq. 9.

The resulting two-wall mPB equation reduces exactly to an integrated form of the PB equation if $\sigma = 0$. The latter has an analytic solution and predicts a repulsive force for all d and ξ [2, 13]. The mPB theory also predicts a weak repulsive force at strong coupling for sufficiently large d , arising from weak repulsions between counterions in the dilute PB-like tails of the one-wall profiles discussed above. On the other hand, at strong coupling and sufficiently small d , core repulsions make it unfavorable for particles in the narrow slit to stack perpendicular to the walls, and counterions will be forced into a *single* 2D layer with characteristic lateral spacing $\tilde{a} \simeq l_w/\sqrt{2}$ fixed by neutrality. To interpolate between this limit and weak coupling we choose $\sigma = \sigma^{2w} \equiv C \min(l_B, l_w/\sqrt{2})$, and take the same value of $C = 0.60$ that we used for the one-wall theory. Since $\tilde{\sigma}_{\min} = C\xi$ at small ξ , the PB approximation is consistent only as $\xi \rightarrow 0$. The mPB theory naturally introduces a crucial new length scale σ_{\min} that allows for a change in the functional form of $n_R(\tilde{z})$ as ξ increases.

Figure 5 compares numerical results of mPB theory [17] to simulation data [13] for strong coupling states. The left graph shows for $\xi = 100$ there is very good agreement between the mPB theory and computer simulations for all widths where simulations can be performed. As shown in the inset, the mPB theory predicts that at still larger widths there is a weak repulsive force between the walls. This reentrant behavior is illustrated more generally in the right graph, which also shows that a minimal coupling strength of $\xi \geq \xi_c \simeq 12$ is needed to get any attraction [13].

The left graph also shows results from the analytic SCA, where $n(\tilde{z})$ is approximated by $n_0(\tilde{z}) \equiv A_0 \exp[-\tilde{\phi}_0^{2w}(\tilde{z}; \tilde{d})]$, with A_0 similarly determined by neutrality. At strong coupling and large d , $\tilde{\phi}_0^{2w}(\tilde{z}; \tilde{d})$ has a deep attractive well near each wall essentially identical to that found near a single wall. However at small enough d the wells from the individual $\tilde{\phi}_0^{1w}$ terms in Eq. 10 begin to overlap and their depth decreases. As $d \rightarrow 0$, $\tilde{\phi}_0^{2w}(\tilde{z}; \tilde{d})$ vanishes for all \tilde{z} in the slit. The SCA fails at large widths, just as it did far from the wall in the

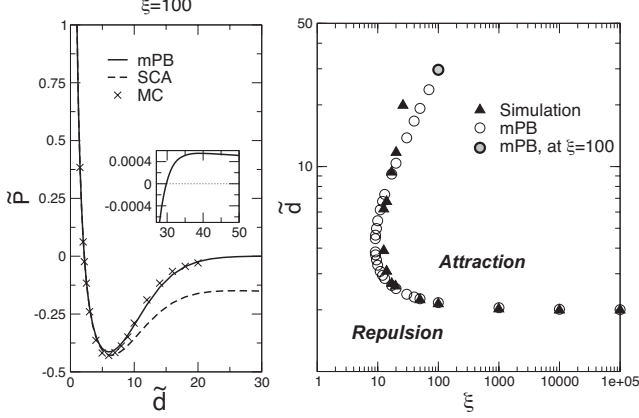


FIG. 5: Left graph: Dimensionless pressure at strong coupling between two equally charged hard walls as a function of width \tilde{d} from [13] compared to predictions from the full mPB theory and the SCA. The inset shows that the mPB theory predicts a weak repulsive force at larger widths. Right graph: Repulsive and attractive forces between two charged walls as a function of width and coupling strength as determined by MC simulations and the mPB theory.

one-wall case, and the reentrant behavior is completely missed. However, it is very accurate at smaller widths and it gives a good description of the location and magnitude of the maximum attractive force.

The formation of the single 2D layer at sufficiently small widths $\tilde{d} < \tilde{\sigma}^{2w}$ plays a key role in producing a strong attractive force. Because of the absence of correlations normal to the walls, the density profile will be relatively constant across the slit. We can use the SCA to describe several features analytically in this regime. The minimum pressure \tilde{P}^* should occur near the largest width $\tilde{d}^* \equiv 2\tilde{z}_m^*$ for which the single 2D layer remains stable, defined by $\tilde{\phi}_0^{2w}(\tilde{z}_m^*; \tilde{d}^*) = 1$. At larger widths there will be higher contact densities as separate 2D layers at each wall begin to form, and the nearly constant profiles at smaller widths will have higher contact densities by normalization. Expanding $\tilde{\phi}_0^{2w}(\tilde{z}; \tilde{d})$ in a Taylor series, we have $\tilde{\phi}_0^{2w}(\tilde{z}; \tilde{d}) = 2\tilde{z}(\tilde{d} - \tilde{z})/(\pi^{1/2}\tilde{\sigma}^{2w})$ to lowest order; higher order terms are negligible for $\tilde{d} \ll \tilde{\sigma}^{2w}$. This implies $\tilde{d}^* = (2\pi^{1/2}\tilde{\sigma}^{2w})^{1/2} \simeq 1.94\xi^{1/4}$, using our expression for $\tilde{\sigma}^{2w}$. Similarly evaluating A_0 , the minimum pressure is $\tilde{P}^* \simeq 3.717/\tilde{d}^* - 1$. When $\tilde{P}^* = 0$ there can be no attractive forces; this determines the minimal coupling strength $\xi_c \simeq 13.48$ and associated critical spacing $\tilde{d}_c^* \simeq 3.717$ needed to get any attraction. Finally, for $\xi \gg \xi_c$ and $\tilde{d} = 2$ we see $\tilde{\phi}_0^{2w}(\tilde{z}; \tilde{d}) \ll 1$, so the constant profile $n_0(\tilde{z}) = 2/\tilde{d}$ is very accurate. Equation 9 then implies that at very strong coupling the transition from strong repulsive to strong attractive forces occurs near $\tilde{d} = 2$, as shown in [12, 13]. All these predictions are in very good agreement with numerical solutions of the mPB theory (and with simulations of

the full and mimic systems, where available) for all strong coupling states, as illustrated in Fig. 5.

Discussion

In strong coupling regimes the short ranged parts of the Coulomb interactions efficiently compete with the other short ranged molecular core interactions and strongly influence pair correlations between neighboring molecules. In LMF theory the choice of σ_{\min} determines the strength and range of these important Coulomb core interactions. They play a key role in inducing an effective attraction between like-charged objects at strong coupling, as illustrated here in Fig. 3 for the correlation functions between like-charged ions in the SAPM, and in Fig. 5 for the osmotic pressure on two like-charged walls. In both cases, strong short ranged forces mainly involving single counterions or a single counterion layer can mediate a strong effective attraction. Such phenomena have traditionally been interpreted as illustrating the “breakdown of mean field theory” and the need for new and more sophisticated approaches. But LMF theory using the simple strong coupling approximation, where only the short ranged parts of the Coulomb interactions are taken into account, provides very accurate results at small and moderate separations. At weak coupling and for long wavelength correlations the averaged effects of the long ranged interactions as determined by the LMF equation are needed as well [6].

LMF theory provides a general conceptual framework that connects and clarifies previous work on systems with both short and long ranged interactions. It has been used to describe liquid-vapor interfaces and wetting and drying transitions for simple fluids [5] and hydrophobic interactions in water [18]. It suggests new and simplified simulation models for general Coulomb systems based on the mimic system that do not require special treatment of periodic boundary conditions. The short ranged intermolecular interactions in the Coulomb mimic system are reminiscent of the truncated interactions used in reaction field methods [19]. But it was not very clear in those approaches how to choose an appropriate cutoff and how to treat nonuniform environments. The determination of σ_{\min} and the effective field in LMF theory provides a way to deal with both problems. We believe the LMF picture will prove useful not only in formal theory, but also for qualitative reasoning and in detailed simulations of biophysical systems.

Detailed results for charged hard walls, including MC simulations of the nonuniform mimic system using both the SCA and the full LMF theory, with important contributions made by Charanbir Kaur and Jocelyn Rodgers, will be presented elsewhere [17]. We are grateful to them and to Michael Fisher for many helpful remarks. We thank J. J. Weis for sending us his simulation data for the SAPM correlation functions. This work was supported by the National Science Foundation through grants CHE01-11104 and CHE05-17818.

-
- [1] Gelbart, W. M., Bruinsma, R. F., Pincus, P. A. & Parsegian, V. A. (2000) *Phys. Today* **53**, 38-44.
- [2] Levin, Y. (2002) *Repts. Prog. Phys.* **65**, 1577-1632.
- [3] Grosberg, A. Y., Nguyen, T. T. & Shklovskii, B. I. (2002) *Rev. Mod. Phys.* **74**, 329-345.
- [4] Boroudjerdi, H., Kim, Y.-W., Naji, A., Netz, R. R., Schlagberger, X. & Serr, A. (2005) *Phys. Repts.* **416**, 129-199.
- [5] Weeks, J. D. (2002) *Annu. Rev. Phys. Chem.* **53**, 533-562.
- [6] Chen, Y.-G., Kaur, C. & Weeks, J. D. (2004) *J. Phys. Chem. B* **108**, 19874-19884.
- [7] Chen, Y.-G. (2004) Ph. D. Thesis, Dept. of Physics, Univ. of Maryland.
- [8] Frenkel, D. & Smit, B. (2002) *Understanding Molecular Simulations* (Academic Press, San Diego).
- [9] Kim, Y. C., Fisher, M. E. & Panagiotopoulos, A. Z. (2005) *Phys. Rev. Lett.* **95**, 195703.
- [10] Weis, J. J. & Levesque, D. (2001) *Chem. Phys. Lett.* **336**, 523-528.
- [11] Wennerstrom, H., Jonsson, B. & Linse, P. (1982) *J. Chem. Phys.* **76**, 4665-4670.
- [12] Moreira, A. G. & Netz, R. R. (2000) *Europhys. Lett.* **52**, 705-711.
- [13] Moreira, A. G. & Netz, R. R. (2002) *Eur. Phys. J. E* **8**, 33-58.
- [14] Rouzina, I. & Bloomfield, V. A. (1996) *J. Phys. Chem.* **100**, 9977-9989.
- [15] Shklovskii, B. I. (1999) *Phys. Rev. E* **60**, 5802-5811.
- [16] Chen, Y.-G. & Weeks, J. D. (2005) *J. Phys. Chem. B* **109**, 6892-6901.
- [17] Rodgers, J., Kaur, C., Chen, Y.-G. & Weeks, J. D. (unpublished)
- [18] Lum, K., Chandler, D. & Weeks, J. D. (1999) *J. Phys. Chem. B* **103**, 4570-4577.
- [19] Hummer, G., Soumpasis, D. M. & Neumann, M. (1994) *J. Phys., Condens. Matter (UK)* **6**, A141-144.